



LAWRENCE  
LIVERMORE  
NATIONAL  
LABORATORY

# ULTRA-COMPACT ACCELERATOR TECHNOLOGIES FOR APPLICATION IN NUCLEAR TECHNIQUES

S. Sampayan, G. Caporaso, Y-J. Chen, V. Carazo, S. Falabella, G. Guethlein, S. Guse, J. R. Harris, S. Hawkins, C. Holmes, M. Krogh, S. Nelson, A. C. Paul, D. Pearson, B. Poole, R. Schmidt, D. Sanders, K. Selenes, S. Sitaraman, J. Sullivan, L. Wang, J. Watson

June 15, 2009

10th International Conference on Applications of Nuclear  
Techniques

Crete, Greece

June 14, 2009 through June 20, 2009

## **Disclaimer**

---

This document was prepared as an account of work sponsored by an agency of the United States government. Neither the United States government nor Lawrence Livermore National Security, LLC, nor any of their employees makes any warranty, expressed or implied, or assumes any legal liability or responsibility for the accuracy, completeness, or usefulness of any information, apparatus, product, or process disclosed, or represents that its use would not infringe privately owned rights. Reference herein to any specific commercial product, process, or service by trade name, trademark, manufacturer, or otherwise does not necessarily constitute or imply its endorsement, recommendation, or favoring by the United States government or Lawrence Livermore National Security, LLC. The views and opinions of authors expressed herein do not necessarily state or reflect those of the United States government or Lawrence Livermore National Security, LLC, and shall not be used for advertising or product endorsement purposes.

# ULTRA-COMPACT ACCELERATOR TECHNOLOGIES FOR APPLICATION IN NUCLEAR TECHNIQUES\*

S. Sampayan, G. Caporaso, Y-J. Chen, V. Carazo<sup>a</sup>, S. Falabella, G. Guethlein, S. Guse<sup>c</sup>, J. R. Harris, S. Hawkins, C. Holmes, M. Krogh<sup>b</sup>, S. Nelson, A. C. Paul, D. Pearson<sup>c</sup>, B. Poole, R. Schmidt<sup>c</sup>, D. Sanders, K. Selenes<sup>d</sup>, S. Sitaraman, J. Sullivan, L. Wang, and J. Watson

*Beam Research Program  
Lawrence Livermore National Laboratory  
P.O. Box 808, L-645  
Livermore, CA 94551*

## Abstract

We report on compact accelerator technology development for potential use as a pulsed neutron source quantitative post verifier. The technology is derived from our on-going compact accelerator technology development program for radiography under the US Department of Energy and for a clinic sized compact proton therapy systems under an industry sponsored Cooperative Research and Development Agreement. The accelerator technique relies on the synchronous discharge of a prompt pulse generating stacked transmission line structure with the beam transit. The goal of this technology is to achieve ~10 MV/m gradients for 10s of nanoseconds pulses and to ~100 MV/m gradients for ~1 ns systems. As a post verifier for supplementing existing x-ray equipment, this system can remain in a charged, stand-by state with little or no energy consumption. We detail the progress of our overall component development effort with the multilayer dielectric wall insulators (i.e., the accelerator wall), compact power supply technology, kHz repetition-rate surface flashover ion sources, and the prompt pulse generation system consisting of wide-bandgap switches and high performance dielectric materials.

## I. INTRODUCTION

We reported on compact accelerator technology being developed for radiography at Lawrence Livermore National Laboratory [1]. This effort, funded, in part, under the US Department of Energy, has as its objective, the production of a 20-30 ns, 2 kA electron beam pulse, at a 10-20 MV/m gradient for portable radiography applications. Successfully meeting such objectives would allow the implementation of an equivalent FXR or DARHT accelerator in a 1-2 meter length structure at a projected cost of less than \$0.50/volt exclusive of the existing development program.

Short pulse variants of this technology for use in cancer therapy and luggage interrogation have also been reported [2, 3]. In these configurations (figure 1 and 2), we use a pulsed ion source and configure the transmission

lines for 1-20 ns pulses to take advantage of the increased surface flashover threshold of the vacuum interface at decreased pulse widths. Further, for extremely short pulses (~1 ns), the accelerator is configured in a traveling wave mode where the dielectric wall is excited along a small portion of the accelerator equivalent to the bunched length of particles [4].

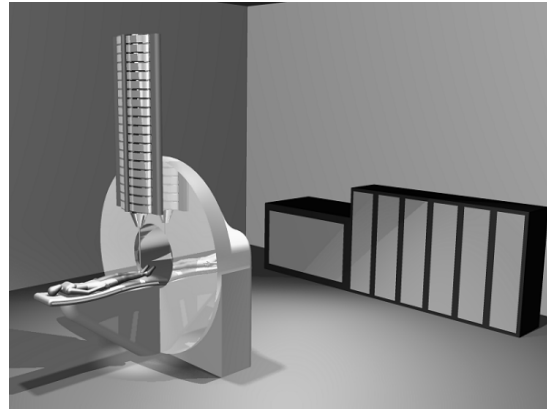


**Figure 1** - Artist rendition of a 250 MeV cancer therapy system [2].

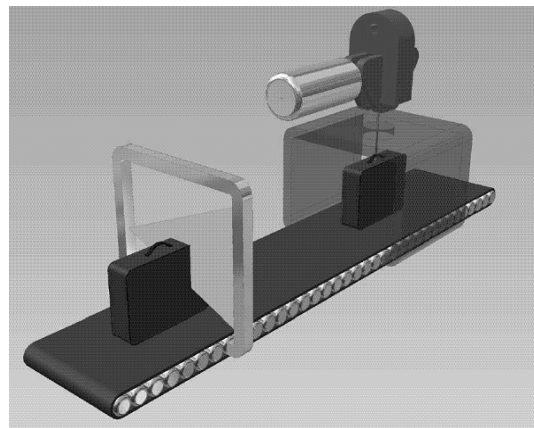


**Figure 2** - High speed CT pre-screener (left) and post verifier concept (right) [3].

Our near term goal is based on oil switching. Although, well proven, it is inadequate for high-repetition rate switching and high reliability commercial applications. As a long term development technology, we are also pursuing linear SiC photoconductive switching in parallel. This technology shows essentially instantaneous recovery and would allow MHz repetition rates within a burst. Such capability would allow a multiframe radiography capability in a compact, inexpensive package for high reliability, continuous applications.

## II. CELL DEVELOPMENT

A DWA prototype cell was designed and built for testing on ETA-II (a 5.5 MeV, 2.0 kA induction LINAC [5]) In the following section, we review the development of the cell components.

### A. Oil Discharge and Photoconductive Switching

Previously, we reported on high pressure gas spark gaps as the means for switching the accelerator [6]. Less than 1 ns simultaneity was demonstrated but short resistive phase time and low inductance was difficult to achieve under the required constraints. Oil switching was subsequently selected because of the increased switch gradient capability that results in faster closure.



Figure 3. Oil switched four-stack Blumlein.

Switch testing was performed in a four stack Duroid based Blumlein system (Figure 3). The system is pulsed-charged and each switch is used in the self-break mode. The particular geometry that proved the most successful was a short rail structure using copper electrodes (Figure 4).

Jitter performance was 1.4 ns for a stack of four Blumleins as was indicated by the break on the charging waveforms. Fast closure times also resulted as indicated by the erection of the voltage on the output (Figure 5).

For commercialization and potential high rep-rate applications, we are also pursuing wide bandgap photoconductive switching (PCSS). Although a unique

application of this technology, these materials have multiple advantages over Si and GaAs. In particular, 6H-SiC and 2H-GaN (band-gaps  $\sim 3 - 3.4$  eV), have high critical field strength (300-400 MV/m), high thermal conductivity, high-saturated electron velocity ( $2.0 - 2.5 \times 10^7$  cm/s) and sufficient carrier density ( $\sim 10^{16} - 10^{17}/\text{cm}^3$ ) to achieve sub-ohm on resistance.

We reported on initial work in this area in our previous paper where we demonstrated the switch capability at 27 MV/m gradient. In that data, the photocurrent essentially followed the laser pulse temporal profile, demonstrating the high recovery rate of the material under high voltage conditions. Our more recent work has focused on measurement of the absorption properties at selected wavelengths, optical switching properties, and achieving higher electric field gradients across the substrate.

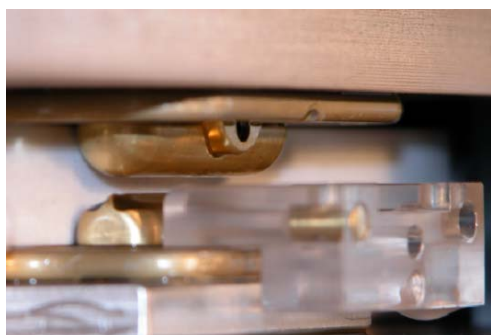


Figure 4. Blumlein oil switch.

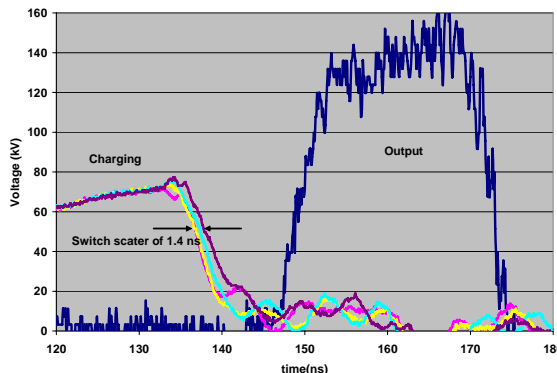


Figure 5. Demonstrated switch jitter (1.4 ns) and four stack Blumlein output.

The cause of the failure at 27 MV/m gradient in our previous work resulted from the discontinuity at the triple junction (i.e., the electrode-substrate-oil junction). In this first proof of concept test, little effort was spent optimizing the high voltage design. Systematic analysis of that region, however, showed a large enhancement ( $\sim \times 10$ ) thus demonstrating the capability of the material at  $\sim 300$  MV/m (Figure 6).

To realize the full capability of the material, we are developing techniques to better manage the enhanced electric field at that junction. Two of the techniques we are pursuing are shown in Figures 7 and 8.

In Figure 7, a cavity is formed in the substrate with a silicon oxide cap. This cavity receives the electrode and the electric field enhancement is graded in the vicinity.

An alternate technique of managing the electric fields is shown in Figure 8. With this particular method, a buried nitride layer is formed below the surface to act as a guard ring near the electrode triple junction.

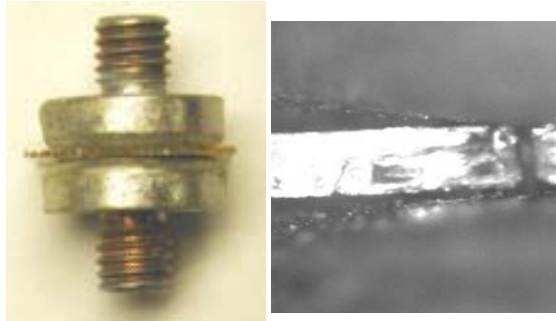


**Figure 6.** Proof of concept switch (left). Cross section of failure at the triple junction interface (right).

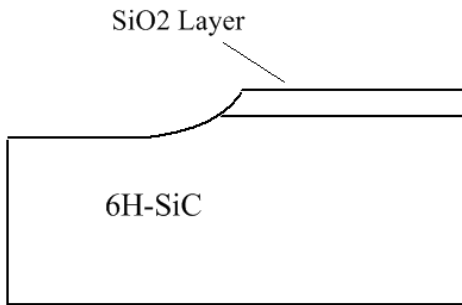


**Figure 7.** Cross section at the SiC dielectric interface near the electrodes using a concavity.

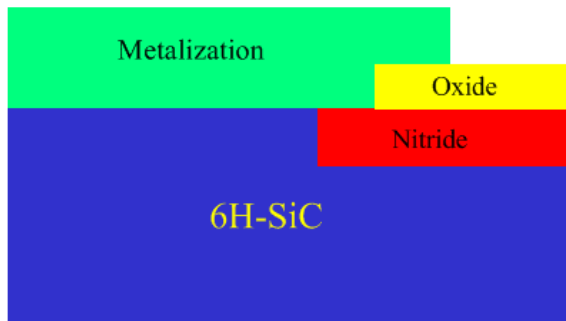


**Figure 8.** Cross section at the SiC dielectric interface near the electrodes using buried layers.

**B. Dielectric Development**

One of the DWA objectives is development of the ability to cast the cell module as a fully integrated unit. This objective was made realizable with the development of high dielectric constant nano-composites made from a polymer resin system and nano-size inorganic particles. The material allows dielectric moldings with complex shapes or effective encapsulation of electrodes and switches. The polymer/particle slurry can be net shape formed into 3-dimensional structures.

In our more recent work, we pursued investigations of the effect of using buried electrodes to minimize enhancement at the triple junction enhancements and the scaling of the breakdown electric field for decreased electrode spacing. A typical sample under test is shown in Figure 9. For these tests, we fabricated multiple samples using a matrix of 16 specimens in a single test sample. In this way we are able assure consistency between each test specimen. The electrode diameter were stainless steel, 2.54 cm diameter with 2 mm spacing.



**Figure 9.** Sample matrix under test.

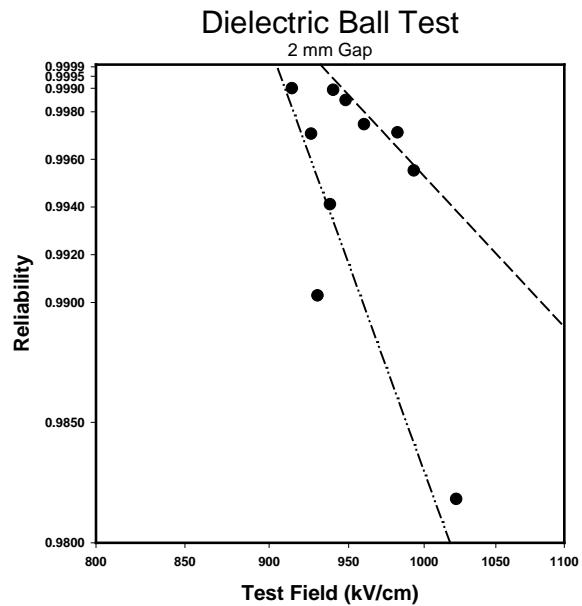


**Figure 10.** Sample reliability.

Our test on these buried electrode samples determined reliability by subjecting each specimen to multiple pulses at given electric fields (Fig. 10). For this test, the electric field is simply the applied voltage divided by gap spacing; the added enhancement that results from spherical electrodes is not applied.

Presumably, the cause of failure in these samples is latent partial discharge eventually resulting in complete failure of the sample. What we also observe in this data is the presence of two specific distributions. The lower distribution of fewer shots on a given sample to achieve breakdown indicates a probable flaw in the material. The upper distribution shows more typical sample behavior. What is evident in this data set is that a slight reduction in electric field results in significant improvement in reliability: high operational reliability should be achievable at fields approaching  $\sim 85$  MV/m.

In a separate test, we also attempted to understand the effect of electrode spacing on breakdown electric field. The result of these tests showed an increase from 92 MV/m gradient at the 2 mm spacing to approximately 400 MV/m gradient at approximately 0.1 mm spacing. This latter data used a slow charging waveform at the elevated fields.

### C. Multi-layer Insulators

We continue to pursue development of High Gradient Insulators (HGIs) for use as the "dielectric wall" of the DWA. These structures are a vacuum insulator composed of alternating layers of metal and dielectric, and have been shown to withstand up to four times the gradient of conventional straight-walled insulators [6]. Although this improvement is similar to that obtained from the standard 45-degree vacuum insulator, the HGI does not have a preferred voltage orientation. This makes it ideal for applications, like the DWA, where it may be subjected to voltage reversals. Our recent work has shown the important role played by high-voltage conditioning in increasing the flashover threshold of HGIs, and demonstrated improved performance obtained by increasing the dielectric layer thickness. We are also investigating how the displacement current through vacuum insulators may affect their dielectric strength under high-gradient, short-pulse conditions.

## III. ACCELERATOR CELL TESTS

We recently performed proof of concept cell testing of a DWA cell on ETA-II. Shown in Figure 11 (top) is the downstream beamline of ETA-II with the prototype cell immediately after a transport solenoid. A  $60^\circ$  analyzing magnet and detector behind the cell is used to determine the added energy gain.

The cell consisted of four separately cast Blumlein structures with self-break oil switches initiating the pulse. Jitter was less than 2 ns (figure 11, lower). Also shown in the figure are four separate multilayer HGI structures

separated by aluminum flanges. This method of assembly was modular which allowed rapid replacement of sections during test. Not shown in the photo are the ferrite isolation cores required to minimize wall currents in the cell housing.

The result of these initial tests are shown in Figure 12. Beam energy measurement as a function of time using spectrometer is shown. The lower trace is the ETA-II electron beam energy without the DWA cell energized. The upper trace is final beam energy with the DWA cell energized. The net energy gain from this particular data set was 3-4 MV/m gradient or approximately one order of magnitude greater than ETA-II.

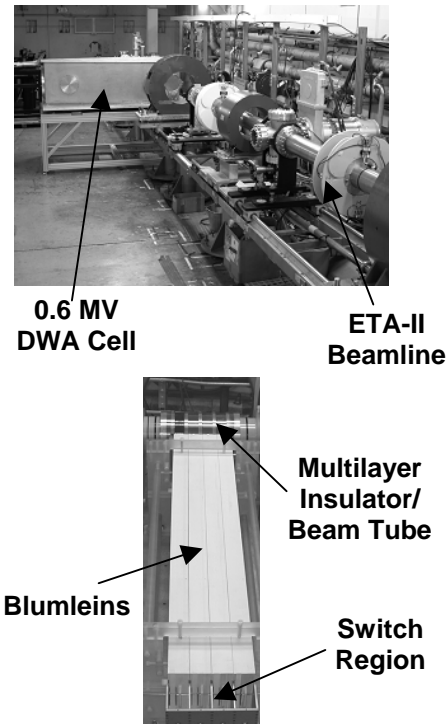


**Figure 11.** DWA prototype cell during installation (upper photo). Blumleins and insulator structure viewed from the switch end of the structure (lower photo).

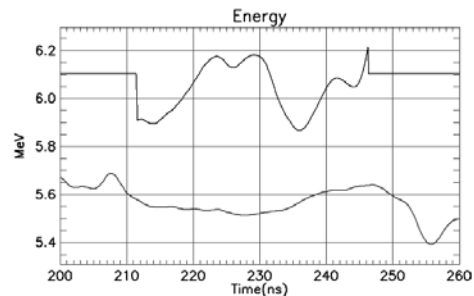


**Figure 12.** Beam energy measurement as a function of time using spectrometer. Lower trace is ETA-II energy without the DWA cell energized. Upper trace is final beam energy with DWA cell energized.

## IV. ION SOURCE TECHNOLOGY

Most ion source technology is large and complex. Further it requires differential pumping to maintain the required pressure for the plasma chamber while maintaining vacuum several orders of magnitude below that for the accelerator. This pressure differential creates a significant outflow of partially ionized low pressure gas through the ion exit aperture in the plasma chamber and extractor electrodes. Typical fields in this region are generally limited to 10s of kilovolts per centimeter. The net result is very low extracted current densities. Thus to create short bunched, high current packets of ions requires bunching of the low current beam.

To avoid such complexities, we are pursuing surface discharge ion sources originally developed by Gow in the thirties. In this technology, hydrated metallic films are used as the electrodes on an insulating substrate. By applying a pulse to these electrodes, a very prompt high density plasma forms from which a high current ion beam (in this case proton's if hydrated and deuterons if deuterated). Because the plasma is transient, very large electric field ( $\sim 200$  kV/cm) can be used in the extractor region to bunch and focus the beam. Further, the system is extremely compact and occupies significantly far less volume that a conventional ion source and buncher system (figure 13).

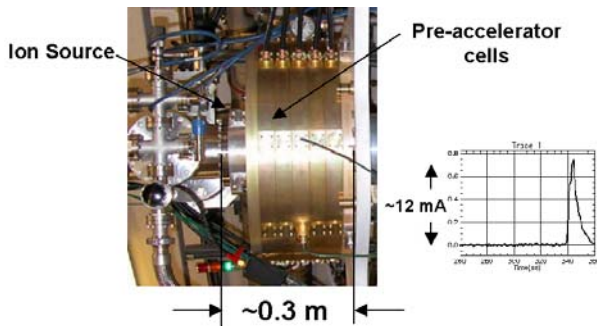


**Figure 13.** Injector for the system. Pulsed protons of 12 mA were extracted during initial tests.

## V. SELECTIVE INTERROGATION DETECTION

The concept we are pursuing is to use conventional x-rays to pre-screen a volume in question and use a pulsed accelerator as the a post verifier to clear suspect voxels.

The pre-screening technique uses a *pixelized* CT technique for speed and agility. In this technique, each x-ray source is maintained at a fixed position around the object and the x-ray cone is rotated around the volume by strobing each pixel in a sequential (i.e., analogous to a marquee sign) or in a semi-sequential manner (Fig. 2). Millisecond slice capture times and mm-sized resolution were reported with such technology [7]. We improve on

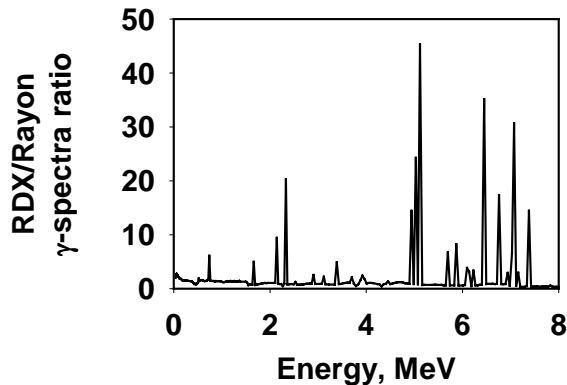
this technique by minimizing beam space charge expansion with the increased electric field gradient capability of our multilayer insulator structures and by exploiting the focusing property resulting from the perturbed local electric fields near the wall [8]. The net result is higher beam current, smaller spot size, and increased resolution. Further, the flexibility of the approach allows increased statistics for more opaque regions by increasing the x-ray spot dwell time.

Selective neutron based interrogation of only high risk volumes within the scanned object is performed with our compact accelerator technology. A material specific gamma spectra results. The accelerator concept is based on the synchronized discharge of stacked, integrated, pulse forming lines (PFLs) arranged along a dielectric wall beam tube that serves as the vacuum interface. Accelerator pulse length is determined by the PFL length. The resulting axial acceleration field is developed along this dielectric wall, hence the name “Dielectric Wall Accelerator” or DWA. As the technique is a non-resonant acceleration method, a single structure can be used for any charge to mass species. Thus, other interrogation reactions such as accelerating protons to generate monoenergetic gammas from the reaction  $^{19}\text{F}(p,\gamma\alpha)\text{O}^{16}$  are possible for fissile and nuclear components (e.g., D, Be, etc., [9]) detection and can be performed in the same structure by only adjusting the synchronization of the pulse timing.

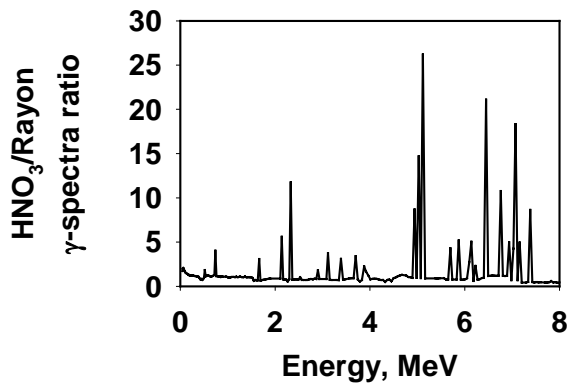
We performed several MCNP calculations to determine the neutron flux and quantitative detection sensitivity requirements for several cases. The model was based on standard carry-on luggage (36 cm high x 56 cm long x 23 cm deep) at a density of  $0.5 \text{ g}\cdot\text{cm}^{-3}$ . The calculations were baselined with a rayon fill ( $\text{C}_{18}\text{S}_{12}\text{Na}_6\text{O}_{10}$ ). Incident neutron energy was 8 MeV and assumed to be collimated to a 5 cm radius cylindrical internal sub-structure approximately 13 cm tall and in the center of the rayon volume. Total volume of the internal structure was approximately  $\sim 1000 \text{ cm}^3$ . One military explosive case was modeled (RDX,  $\text{C}_3\text{H}_6\text{N}_6\text{O}_6$ ) and components consisting of glycerin ( $\text{C}_3\text{H}_8\text{O}_3$ ), nitric acid ( $\text{HNO}_3$ ), and hydrogen peroxide ( $\text{H}_2\text{O}_2$ ). The military explosive, RDX, was chosen because of the similarity in density to wax and would represent an unresolved alarm and manual inspection requirement if stand alone CT detection techniques were used. To determine the detectability of hydrogen peroxide, the data was compared against water. Detector efficiency was not considered in these models and all gammas within  $4\pi$  steradians were tallied.

The results of these models are shown in Figure 14. Typical gamma production efficiency is  $\sim 10^{-5} \gamma/n$ . To determine detectability (i.e., percent above the nominal rayon fill), the ratio of the gamma spectra for the specified material sub-structure within the rayon volume was compared to the gamma spectra for the baseline rayon only case. These ratios are shown in Figures 14a through 14c. The most easily detected material is RDX in which

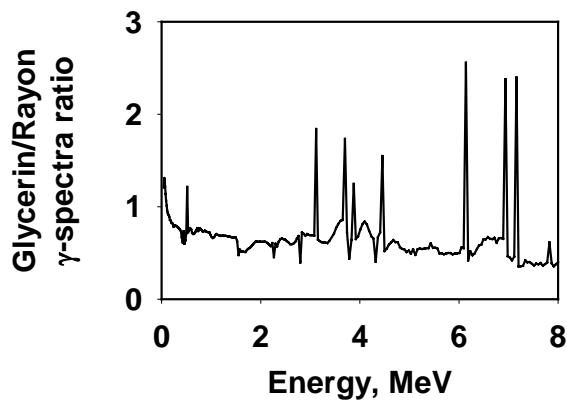
the prominent peaks vary from approximately 5 to 45 above the nominal rayon background. Nitric acid is the second most easily detected substance with ratios of 2 to 25. Finally glycerin, is detectable at ratios to 2.5.



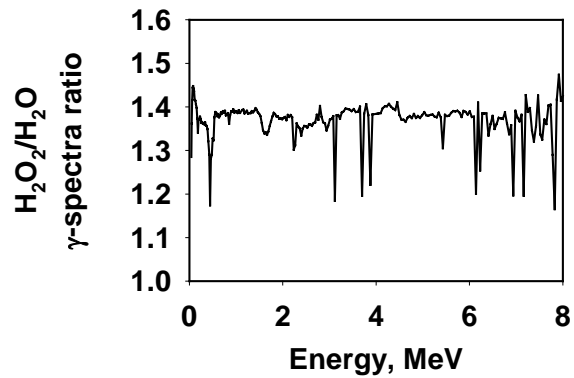
(a) RDX/Rayon



(b) Nitric Acid/Rayon



(c) Glycerin/Rayon



(d) Hydrogen Peroxide/Water

**Figure 14.** Detection ratios for various materials.

Hydrogen peroxide shows a similar ratio above the rayon background, but is shown compared directly to water because of obvious similarities (Figure 14d). In this plot, the ratio of the gamma spectra of the hydrogen peroxide sub-structure within the rayon volume to the gamma spectra of the water sub-structure within the rayon volume is shown. In this comparison, about a 20% difference in prominent peaks results from the hydrogen peroxide to water ratio.

Each of these examples shows good detectability in that each selective interrogation spectra is significantly above the “routine” rayon spectra. Additionally, in the last model, peroxide is also differentiable from water.

## VI. SUMMARY

We performed component development for a prototype DWA accelerator cell. The cell was tested on ETA-II using a magnetic spectrometer. The gradient achieved during these tests was approximately 3-4 MV/m. We have described a concept that uses a high speed, pixelized CT scanner as a pre-screener. Only potential threats are quantitatively probed as required with neutrons or mono-energetic gamma rays. Object dose is therefore minimized. We have performed proof of concept experiments with the pixelized CT scanner and are continuing to test and integrate accelerator components. We are presently integrating and testing a cell to 12 MV/m. Finally, our MCNP calculations show good detectability of military and multi-part component liquids threat systems.

## VII. REFERENCES

\*\*This work performed under the auspices of the U.S. Department of Energy by Lawrence Livermore National Laboratory under Contract DE-AC52-07NA27344. *Patents Pending.*

a) MMech, State College, PA 16803

b) University of Missouri, Rolla, MO 65409, USA.

c) CPAC Inc., Livermore, CA 94550

d) TPL, Inc., Albuquerque, NM 87109, USA

- [1] S. Sampayan, et. al. "Development of Compact Pulsed Power for the Dielectric Wall Accelerator," in Proceedings of the 2006 Power Modulator Symposium, Washington, DC, May 14-18, 2006.
- [2] G. J. Caporaso, et.al. "Compact Accelerator Concept for Proton Therapy," accepted for publication in Nuclear Instruments and Methods in Physics Research B.
- [3] S. E. Sampayan, et. al. "Applications of Ultra-Compact Accelerator Technology for Homeland security," accepted for publication in Nuclear Instruments and Methods in Physics Research B.
- [4] B. R. Poole, et. al., "Particle Simulations of a Linear Dielectric Wall Proton Accelerator," in proceedings of the 2007 Particle Accelerator Conference, Albuquerque, NM, June 25-29, 2007.
- [5] J.T. Weir, et. al., "Improved ETA-II Accelerator Performance," in proceedings of the 1999 Particle Accelerator Conference, New York, NY, March 29-April 2, 1999.
- [6] S. E. Sampayan, P. A. Vitello, M. L. Krogh, and J. M. Elizondo, "Multilayer High Gradient Insulator Technology," IEEE Trans. Dielectr. Electr. Insul., Vol. 7, No. 3, pp. 334-339, June 2000.
- [7] K. Hori, T. Fujimoto, and K. Kawanishi, IEEE Trans on Nucl. Sci., v. 45 (4), 2089-2094 (1998).
- [8] J.G. Leopold, U. Dai, Y. Finkelstein, and E. Weissman, IEEE Trans. Dielectrics Elect. Insul. v. 12 (3), 530-536, (2005).
- [9] B. J. Micklich, D. L. Smith, T. N. Massey, D. Ingram, and A. Fessler, "FIGARO: Detect-ing Nuclear Material using High-Energy Gamma Rays from Oxygen," in Applications of Accelerators in Research and Industry - 16th Int'l Conference., edited by J. L. Duggan and I. L. Morgan, AIP (2001).